

# **inTformer: A Time-Embedded Attention-Based Transformer for Crash Likelihood Prediction at Intersections Using Connected Vehicle Data**

## **B.M. Tazbiul Hassan Anik**

Graduate Research Assistant  
University of Central Florida  
4000 Central Florida Blvd Orlando FL 32816  
Email: tazbiul.hassan@knights.ucf.edu

## **Zubayer Islam**

Postdoctoral Scholar  
University of Central Florida  
4000 Central Florida Blvd Orlando FL 32816  
Email: Zubayer.Islam@ucf.edu

## **Mohamed Abdel-Aty**

Pegasus Professor and Trustee Chair  
Department of Civil, Environmental and Construction Engineering  
University of Central Florida  
4000 Central Florida Blvd Orlando FL 32816  
Email: M.aty@ucf.edu

## **ABSTRACT**

The real-time crash likelihood prediction model is an essential component of the proactive traffic safety management system. Over the years, numerous studies have attempted to construct a crash likelihood prediction model in order to enhance traffic safety, but mostly on freeways. In the majority of the existing studies, researchers have primarily employed a deep learning-based framework to identify crash potential. Lately, Transformer has emerged as a potential deep neural network that fundamentally operates through attention-based mechanisms. Transformer has several functional benefits over extant deep learning models such as Long Short-Term Memory (LSTM), Convolution Neural Network (CNN), etc. Firstly, Transformer can readily handle long-term dependencies in a data sequence. Secondly, Transformers can parallelly process all elements in a data sequence during training. Finally, a Transformer does not have the vanishing gradient issue. Realizing the immense possibility of Transformers, this paper proposes inTersection-Transformer (inTformer), a time-embedded attention-based Transformer model that can effectively predict intersection crash likelihood in real-time. The proposed model was evaluated using connected vehicle data extracted from INRIX and Center for Advanced Transportation Technology (CATT) Lab's Signal Analytics Platform. The data was parallelly formatted and stacked at different timesteps to develop nine inTformer models. The best inTformer model achieved a sensitivity of 73%. This model was also compared to earlier studies on crash likelihood prediction at intersections and with several established deep learning models trained on the same connected vehicle dataset. In every scenario, this inTformer outperformed the benchmark models confirming the viability of the proposed inTformer architecture.

**Keywords:** Connected Vehicles, Transformer, Intersection Safety, Real-Time Crash Likelihood

## INTRODUCTION

Intersections are potentially hazardous crash zones with complex traffic operating attributes. According to the Fatality Analysis (FARS) database, approximately 25% (9634) of all fatal crashes in the United States in 2021 are intersection-related. Even at the peak of Covid-19 in 2020, the share of intersection-related fatal crashes in the United States was about 25% (8824) per FARS database. Given this persistent safety-critical state of intersections, researchers have made significant efforts in the previous few decades to improve safety conditions at intersections. Though most intersection safety studies so far have focused on identifying potential features that cause crashes at intersections (Lee et al., 2017; Wu et al., 2021; Yuan & Abdel-Aty, 2018), recent advancements in proactive traffic management systems have widened the scope to improve traffic safety at intersections from multi-other dimensions (Hossain et al., 2019; Shi & Abdel-Aty, 2015).

Real-time crash likelihood prediction is an important component of proactive traffic safety management systems: it uses real-time data to anticipate crash likelihood for the next short period of time (e.g., 5, 10, 15 minutes). Numerous studies have been conducted to date in order to construct realistic and usable real-time crash prediction models for various road segments such as freeways (Abdel-Aty et al., 2023; You et al., 2017; Yu & Abdel-Aty, 2014; Q. Zheng et al., 2021), arterials (Li et al., 2020; Theofilatos, 2017; Yuan et al., 2018), and intersections (Kidando et al., 2022; Yuan et al., 2019, 2021). Unfortunately, research on crash likelihood prediction at intersections is few in comparison to other road segments. This is because the traffic environment at intersections is much more complex, and only simple traffic flow characteristics at intersections cannot capture this complication. For the effective development of real-time crash prediction models at intersections, rich and exhaustive data exhibiting traffic flow mechanism at intersections are essential.

With the installation of various intelligent transportation systems, enormous real-time traffic data is now available via fixed sensors, on board sensors and automatic vehicle identification devices (Ahmed & Abdel-Aty, 2012; Li et al., 2020; Shi et al., 2016). So far, numerous types of data from various sources have been investigated with the purpose of predicting crash likelihood in real-time at intersections (Ali et al., 2023; Kidando et al., 2022; Yuan et al., 2019, 2021; L. Zheng & Sayed, 2020). The majority of the data analyzed in the existing studies came from roadside sensors. Though sensor data has enormous potential to aid in the deployment of proactive management strategies, such as real-time crash likelihood prediction models at intersections, it also has limitations. To begin, sensor data does not always provide complete coverage of intersections. Second, roadside sensors are frequently costly and laborious to set up and deploy. Thirdly, roadside sensors are susceptible to hardware failure or network outages, resulting in data loss and significant maintenance expenses. All of these sensor constraints highlight the need for an alternate intersection-related data source that provides maximum coverage of intersections while requiring minimal setup cost and maintenance.

Vehicle-based data has recently gained popularity because of its wide coverage, low cost, and minimal maintenance. The network-enabled on-board units (OBUs), which enable vehicles to

communicate with external agents in real-time, are a well-known source of vehicle-based data. At the moment, most modern vehicles are equipped with OBUs, allowing them to communicate with their surroundings. Nonetheless, vehicles without OBUs, particularly those that operate in app-based ride-sharing services, can generate vehicle-based data as well. These data-generating vehicles, also known as connected vehicles, as a whole, represent a possible source of appropriate information required for infrastructure-free real-time crash likelihood prediction. Nevertheless, assembling connected vehicle data can be challenging at times. At the industrial level, multiple organizations assemble, and archive connected vehicle data for analysis and visualization. Signal Analytics, primarily operated by INRIX, is one such platform that archives vehicle-based data representing the traffic dynamics at intersections. According to the Regional Integrated Transportation Information System (RITIS), Signal Analytics acquires data from connected vehicles, which account for over 8% of the moving traffic stream. Since connected vehicles are projected to saturate the market soon, Signal Analytics is a viable option for real-time crash likelihood prediction. Regardless of this possibility, to the best of the authors' knowledge, no studies on real-time crash likelihood prediction at intersections so far used vehicle-based data sourced from INRIX and Center for Advanced Transportation Technology (CATT) Lab's Signal Analytics platform for modeling intersections' safety.

From a methodological standpoint, there are two separate ways to predict crash likelihood in real-time: statistical-based and machine learning-based. Although statistical methods are generally focused on identifying possible features that influence crash likelihood, several methods, including logistic regression, conditional logit model, Bayesian random effect logit, etc., have also contributed to real-time crash likelihood prediction. Unfortunately, statistical methods have substantial assumptions and dependencies on data distribution and preparation techniques, which frequently degrade crash likelihood prediction aptitude (Abdel-Aty & Wang, 2006; A. J. M. M. U. Ahmed et al., 2017; Ahsan et al., 2021; F. Guo et al., 2010; Hasan et al., 2022; Lee et al., 2017; Rashid et al., 2018). Machine learning approaches, on the other hand, have strong prediction competencies without the need for any assumptions. Hence, several researchers have applied traditional machine learning methods like support vector machines (Yu & Abdel-Aty, 2013), random forest (Lin et al., 2015; You et al., 2017), etc., to predict crash likelihood. However, the traditional machine learning algorithms frequently fail to handle high-dimensional data (S. Guo et al., 2019). Lately, deep learning algorithms have attracted a lot of attention from traffic safety researchers because of their ability to efficiently work with high-dimensional data. Deep learning is basically a subset of machine learning that focuses on deep neural networks.

Several previous studies have successfully employed deep learning frameworks to predict crash likelihood in real-time. Basso et al. (2021), for example, presented a concatenated convolution neural network (CNN) for predicting real-time crash likelihood in Santiago, Chile freeways. Yu et al. (2020) combined geometry and traffic data gathered from loop detectors on freeways in Shanghai, China, to construct a CNN model with a refined loss function for predicting real-time crash likelihood. Theofilatos et al. (2019) analyzed traffic data from two freeways in Shanghai, China, to compare the predictive performance of multiple machine-learning and deep-

learning models, concluding that deep-learning models outperform machine-learning models in real-time crash prediction. To predict real-time crash likelihood on freeways in Florida, Zhang & Abdel-Aty (2022) proposed a bidirectional long short-term memory (LSTM) model with two convolutional layers. Li et al. (2020) developed an LSTM-CNN model for predicting the likelihood of crashes on arterials in Orlando, Florida. Additionally, deep-learning models can be used to augment crash data. For instance, Islam et al. (2021) developed a variational autoencoder to generate crash data for the prediction of crash likelihood. While deep learning models surpassed various traditional machine learning models and statistical models in prediction accuracy in all of the aforementioned studies, the explorations were largely performed on highways and arterials. Deep learning methods have rarely been used to forecast crash likelihood at intersections. To the best of the authors' knowledge, only Yuan et al. (2019) implemented a deep learning technique, the LSTM model, for predicting real-time crash likelihood at signalized intersections. The authors achieved a sensitivity of 60.67%, and a false alarm rate of 39.33%, in favor of the LSTM over the conditional ordered logit model.

In addition to the existing deep neural networks, lately, Transformers have received significant interest among researchers in various fields. The Transformer model, introduced by Vaswani et al. (2017), is an attention-based model, devoid of recurrence and convolutions. Transformers were originally designed for machine translation, but they have since extensively reshaped the field of natural language processing (Devlin et al., 2018; Vaswani et al., 2017) and even extended their reach to other domains such as computer vision (Abdelraouf et al., 2022), speech detection (Gulati et al., 2020). Structurally, Transformer learns dependencies in sequential data by leveraging the attention mechanisms that allow the algorithm to focus directly on any part of the sequence, regardless of the distance. Nevertheless, this attribute is missing in sequential algorithms like LSTM. Hence, unlike Transformer, LSTM often fails to handle long-range dependencies in a sequence, resulting in information loss over very long sequences. Another advantage of Transformer over LSTM is, Transformer, avoiding sequential processing like LSTM, can parallelly process all elements in the input sequence during training. Although this parallel processing significantly optimizes the computation time of Transformer, the inability of sequential processing, however, frequently makes it difficult for Transformer to understand dependencies and interactions in temporal sequence data in time series analysis. To circumvent this sequential constraint, researchers have proposed numerous Transformer variants that may effectively execute time series tasks (Xu et al., 2020). Most of the proposed architectures embedded new layers or modified existing layers to precisely capture the temporal order of the sequence in the time series data, resulting in enhanced performance. Unfortunately, despite the immense potential of Transformers in time series analysis, no studies have yet applied Transformer in real-time crash likelihood prediction, which is fundamentally a time series classification task.

In summary, by reviewing existing literatures on real-time crash likelihood prediction three research gaps can be identified. First, to the best of the author's knowledge, connected vehicle data accounting for intersection traffic dynamics have not yet been explored for real-time crash likelihood prediction at intersections. Second, no studies have applied Transformer model to

predict crash likelihood in real-time for any roadway segments including intersections. Third, to date there are no viable models that have been developed to predict crash likelihood at intersections in real-time. To fill in these gaps, this study contributed as follow:

- developed a time-embedded Transformer model, named intersection-Transformer (inTformer), purposed to predict real-time crash likelihood at intersections.
- explored connected vehicle data sourced from INRIX and CATT Lab's Signal Analytics platform for crash likelihood prediction at intersections.

## DATA DESCRIPTION AND PREPARATION

### Data Description

In general, the frequency of crashes at a location is a direct reflection of the riskiness of the location, i.e., the more frequently crashes occur, the more dangerous the location. Given this fact, this paper selected six intersections in Tampa and two in Orlando, Florida, as shown in Table 1. For the period July 2021 to June 2022, three types of datasets were collected in this study: (a) crash data from Signal Four Analytics (S4A); (b) connected vehicle data from INRIX and CATT Lab's Signal Analytics; (c) weather data.

**Table 1. Selected Intersections with Crash Count**

Intersection Name	Latitude	Longitude	Crash Count
East Hillsborough Avenue	27.99616	-82.45416	75
West Brandon Boulevard & Brandon Town Center Drive	27.93939	-82.32389	66
East Dr. Martin Luther King Jr Boulevard & North Marguerite Street	27.98149	-82.45422	60
Polk City Road & US 27	28.12132	-81.6397	57
East Hillsborough Avenue & North Nebraska Avenue	27.99607	-82.45114	54
Glen Este Boulevard & US 27	28.12499	-81.6397	51
East Dr. Martin Luther King Jr Boulevard & US 301	27.98146	-82.36012	50
West Columbus Drive & North Dale Mabry Highway	27.96679	-82.50551	49

### Crash Data

This paper employed crash data retrieved from the Signal Four Analytics (S4A) database. S4A is a data analytics platform that provides crash data and analytics solutions to organizations in the transportation industry. The crash data from S4A includes information on the crash timing, type, severity, and location, as well as other factors such as weather, road conditions, etc. In this research,

all crashes that occurred at the study intersections or road sections influenced by intersections (within 250 feet of intersections (Yuan et al., 2019; Yuan & Abdel-Aty, 2018)) between July 2021 and June 2022 were collected. Using QGIS, the collected crashes were then matched with the respective intersections. In total, 462 crashes were identified within 250 feet of all study intersections.

### ***Connected Vehicle Data***

In this study, the traffic data were collected from the Signal Analytics platform. Signal Analytics is the product of a collaboration between INRIX and the Center for Advanced Transportation Technology (CATT) Lab that focuses on capturing the traffic dynamics at intersections. Signal Analytics collects real-time traffic data from connected vehicles. To do so, each sampled vehicle is assigned to one of the 230-meter zones (one for each approach direction), as shown in Figure 1. Once a connected vehicle enters the 150-meter ‘Shared Approach Zone’ in Figure 1, Signal Analytics begins collecting pings from the vehicle every 3 to 5 seconds until the vehicle exits via the 80-meter ‘Right,’ ‘Through,’ or ‘Left,’ zone. Following ping collection, the Signal Analytics platform estimates travel times, control delays, and whether a vehicle is considered to have stopped within the intersection. In total, the platform stores aggregated information on nine different features, namely, split failure count (SFC) and split failure percentage (SFP), travel time maximum (TTM) and travel time average (TTA), control delay maximum (CDM) and control delay average (CDA), approach speed maximum (ASM) and approach speed average (ASA), and percent (arrival) on green (POG) every 15 min.

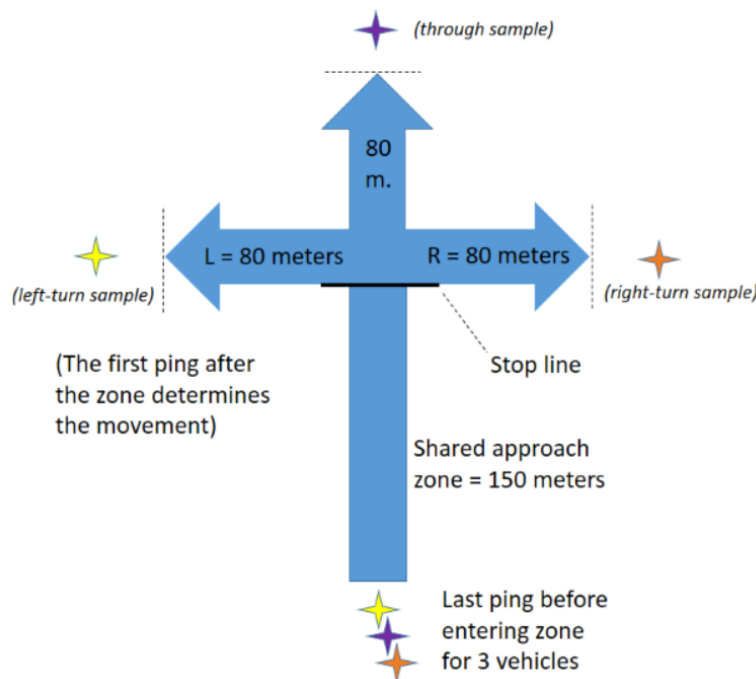


**Figure 1. Intersection Analysis Zone (Signal Analytics Help)**

A split failure happens when the green signal time fails to meet the vehicle volume demand during one cycle, i.e., if a driver has to wait for more than one cycle at a traffic light. The trip time is based on the time it takes each observed vehicle to traverse the intersection's 230-meter analysis zone. The control delay is the difference between the observed and reference travel times; the reference travel time is the 5<sup>th</sup>-percentile fastest travel time recorded for each intersection approach direction. The approach speed is the calculated speed of each sampled vehicle while traversing the 150-meter approach zone. Finally, the percentage of observed vehicles that passed through the crossing without stopping is designated as the POG. POG can be expressed mathematically as follows (Equation 1):

$$POG = \frac{Vehicle\ Count:Total - Vehicle\ Count:Stopped}{Vehicle\ Count:Total} \times 100 \quad (1)$$

### ***Weather Data***

Six weather-related features (temperature, relative humidity, wind speed, precipitation, visibility, and weather type) were retrieved using weather API from Visual Crossings. The API provides GPS location-specific weather information by triangulating data from nearby weather stations as well as weather radars.

## **Data Preparation**

### ***Intersection Zoning***

The traffic operation mechanism at intersections is very intricate. The way traffic behaves within intersections differs significantly from the way traffic approaches intersections. As a result, the crash occurrence dynamics at intersections frequently differ depending on whether the crash occurs within the intersection or on the approach to the intersection. To analyze such crash complexity at intersections, this study segmented the intersection area into two zones: within-intersection zone and approach zone, as illustrated in Figure 2. The boundary of the within-intersection zone is simply the rectangular zone at the intersection that connects all of the approaches. To determine the boundary of the approach zone, prior studies were followed (Yuan et al., 2019; Yuan & Abdel-Aty, 2018). The existing studies indicated that intersections have a radial influence of 250 feet from their center. Hence, in this study, the approach road segments falling within the intersection's influence margin, i.e., within 250 feet, were designated as the approach zone.



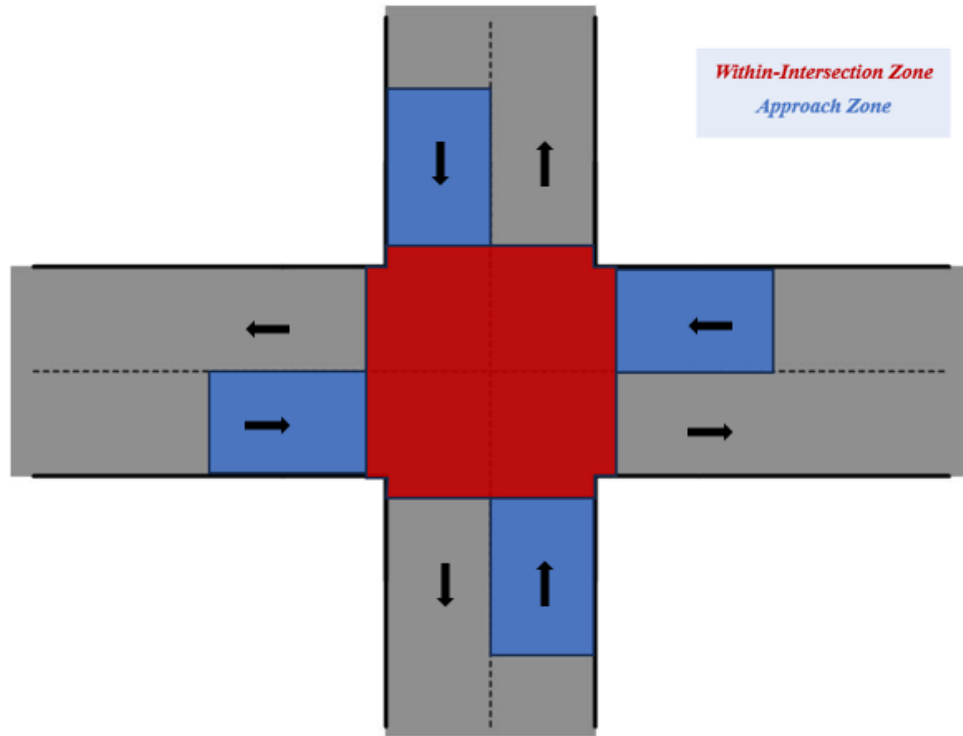


**Figure 2. Intersection Zoning**

### ***Crash Labeling***

This research assumed real-time traffic and weather data 15-30 min before the occurrence of the crash incident as potential crash-contributing features (Cheng et al., 2022; Yuan et al., 2018). Thus, if a crash happened, say, at 10:50, data from 10:30 to 10:45 were categorized as 1, indicating that a crash will occur within the following 15-30 minutes (see Figure 3). All other timestep observations were designated as 0, i.e., non-crash event. Furthermore, following previous studies (Li et al., 2022; Li & Abdel-Aty, 2022), data within two hours after the crash were removed in this research since a crash event can induce turbulence in traffic conditions.

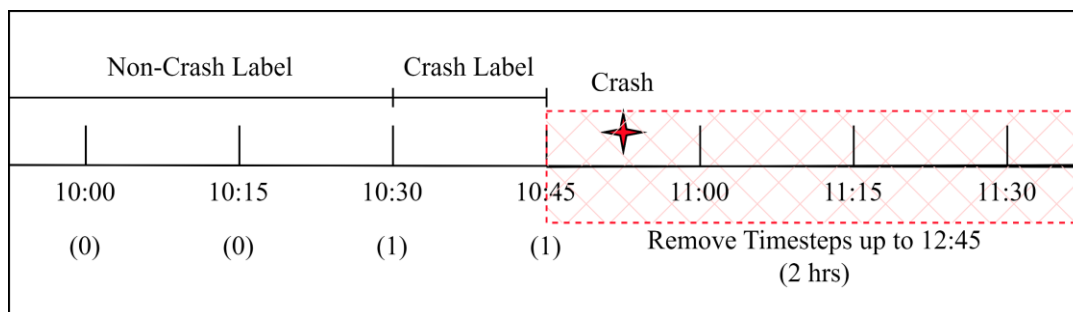


**Figure 3. Crash Labeling**

### ***Direction Nomenclature***

Typically, the traffic operation mechanism at an intersection differs depending on the approach direction of travel. This change in operation mechanism can also take place for the same approach direction at different intersections. Since this study develops the crash likelihood prediction model using 8 different intersections (6 four-legged and 2 three-legged), it is essential to organize the dataset in a way that ensures that approaches with almost identical traffic dynamics fall into the same feature group. Hence, to establish such data formatting, this study adopted the direction nomenclature proposed by Yuan & Abdel-Aty (2018). In accordance with the nomenclature, the intersection approaches were renamed ‘A,’ ‘B,’ ‘C,’ and ‘D,’ to make all features from different approaches comparable for each crash and non-crash event. More specifically, the “A” approach denotes the approach that contributed the most to the crash event (i.e., the direction of the at-fault vehicle), and the “B” approach denotes the “A” approach’s left-side approach. Similarly, the “C” and “D” approaches proceed in a clockwise direction (see Figure 4). Each crash and non-crash event within the intersections were thus represented using real-time traffic parameters derived from all intersection approaches.

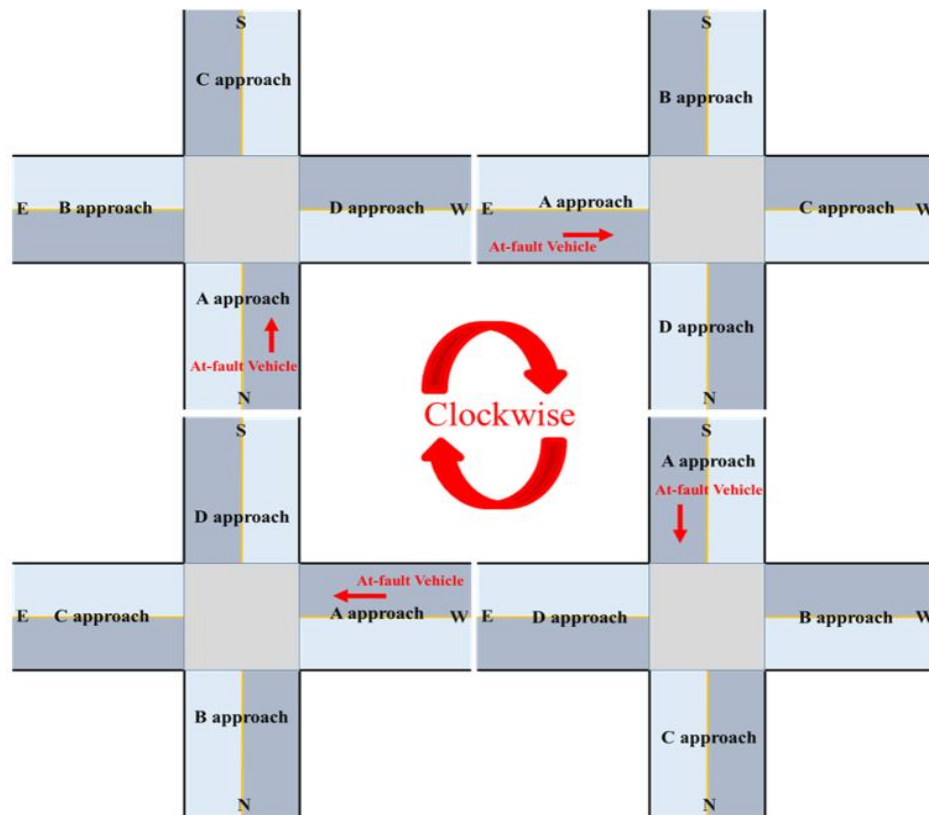


**Figure 4. Direction Nomenclature** (Yuan & Abdel-Aty, 2018)

### ***Data Formatting***

In this study, real-time traffic data from the Signal Analytics archive, which is updated every 15 minutes, were retrieved for all intersection approaches. Using the retrieved raw traffic data, a total of 1,051,200 observations ( $30 ((6 \text{ four-legged intersection} \times 4 \text{ approaches}) + (2 \text{ three-legged intersections} \times 3 \text{ approaches})) \text{ approaches} \times 365 \text{ days} \times 24 \text{ hours} \times (60 \text{ minutes}/15 \text{ minutes}))$ ) were generated, where each observation corresponds to the traffic features of every approach at an intersection over a span of 15 minutes. The generated observations were then formatted using the procedure explained in the ‘Direction Nomenclature’ section. The formatting assured that traffic features from all approaches to an intersection were captured in each observation. More specifically, after data formatting, each observation not only encompassed traffic features of the approach it initially symbolized before formatting, but also the traffic features of all the other remaining approaches. This method of data formatting, however, led to feature duplication problem, since all observations at a specific step in time at an intersection concurrently included traffic features from all approaches. To address this issue, for every timestep at an intersection, only one observation was retained, and the rest were discarded. Following the retention and discarding of data, a total of 280,320 observations were identified. Next, the weather data was matched with each retained observation by taking intersection location and time into account.

The aforementioned approach of data formatting enables the implementation of the real-time model in the context of proactive management and the possibility of devising real-time countermeasures through an adaptive signal control’s Signal and Phase Timing (SPaT) adjustment. Overall, the data formatting led to numerous features. Hence, for illustration purposes, the summary statistics of the traffic characteristics of only approach “A,” and the weather characteristics, for the entire dataset, is depicted in Table 2.

**Table 2. Feature Descriptive Statistics**

Feature	Description	Unit	Mean(Std)	(Min, Max)
<i>ASA L A</i>	Average Speed for Left-Turning, Through, and Right-Turning Vehicles at Approach ‘A’	mph	30.13(5.43)	(11.0, 77.0)
<i>ASA T A</i>			34.87(7.2)	(9.0, 103.0)
<i>ASA R A</i>			31.89(5.29)	(6.0, 102.0)
<i>ASM L A</i>	Maximum Speed for Left-Turning, Through, and Right-Turning Vehicles at Approach ‘A’	mph	31.39(5.68)	(11.0, 78.0)
<i>ASM T A</i>			42.26(11.85)	(9.0, 147.0)
<i>ASM R A</i>			33.34(5.51)	(6.0, 100.0)
<i>TTA L A</i>	Average Travel Time for Left-Turning, Through, and Right-Turning Vehicles at Approach ‘A’	second	71.53(45.85)	(8.0, 532.0)
<i>TTA T A</i>			45.32(34.32)	(5.0, 500.0)
<i>TTA R A</i>			32.71(21.8)	(7.0, 413.0)
<i>TTM L A</i>	Maximum Travel Time for Left-Turning, Through, and Right-Turning Vehicles at Approach ‘A’	second	82.16(55.24)	(8.0, 556.0)
<i>TTM T A</i>			68.59(43.11)	(5.0, 570.0)
<i>TTM R A</i>			37.52(27.9)	(7.0, 489.0)
<i>CDA L A</i>	Average Control Delay for Left-Turning, Through, and Right-Turning Vehicles at Approach ‘A’	second	57.94(45.0)	(1.0, 378.0)
<i>CDA T A</i>			34.58(32.39)	(0.0, 491.0)
<i>CDA R A</i>			17.37(21.83)	(0.0, 395.0)
<i>CDM L A</i>	Maximum Control Delay for Left-Turning, Through, and Right-Turning Vehicles at Approach ‘A’	second	68.4(54.3)	(1.0, 543.0)
<i>CDM T A</i>			57.83(43.04)	(1.0, 559.0)
<i>CDM R A</i>			22.27(28.01)	(1.0, 473.0)
<i>SFC L A</i>	Count of Split Failure for Left-Turning, Through, and Right-Turning Vehicles at Approach ‘A’	-	0.09(0.37)	(0, 8)
<i>SFC T A</i>			0.02(0.19)	(0, 9)
<i>SFC R A</i>			0.04(0.23)	(0, 7)
<i>SFP L A</i>	Percentage of Split Failure for Left-Turning, Through, and Right-Turning Vehicles at Approach ‘A’	%	3(12)	(0, 100)
<i>SFP T A</i>			1(5)	(0, 100)
<i>SFP R A</i>			1(6)	(0, 100)
<i>POG L A</i>	Percentage of Left-Turning, Through, and Right-Turning Vehicles Arrived on Green at Approach ‘A’	%	22(32)	(0, 100)
<i>POG T A</i>			54(36)	(0, 100)
<i>POG R A</i>			69(34)	(0, 100)
<i>Temperature</i>	Dry-bulb Temperature	Fahrenheit	74.82(11.19)	(41.5, 95.0)
<i>Relative Humidity</i>	Relative Humidity	%	68.51(17.56)	(20.6, 100)
<i>Wind Speed</i>	Speed of the Wind	mph	5.89(3.73)	(0.0, 19.9)
<i>Precipitation</i>	Amount of Precipitation	inches to hundredths	0.0(0.04)	(0.0, 0.72)
<i>Visibility</i>	Horizontal Distance an Object can be Seen	miles	9.56(1.11)	(0.6, 9.9)
<i>Conditions</i>	Normal Weather: 0, Abnormal Weather: 1	-	0.18(0.38)	(0, 1)

Here, A: Approach “A,” L: Left-Turn, T: Through, and R: Right-Turn.

Note: Table 2 only depicts Approach “A” data. The final dataset, however, includes data from all approaches.

## ***Crash Integration***

In this study, crashes were integrated simultaneously with the formatted traffic and weather datasets in three distinct ways: within-intersection integration, approach integration, and joint integration. It should be noted that in each form of integration, the labeled crash data were separately combined with the formatted 280,320 observations of traffic and weather data depending on intersection location, time of day, and approach direction.

### ***Within-Intersection Integration***

In this form of integration, crashes occurring only in within-intersection zone of all the subject intersections were used. Out of the 432 extracted crashes from S4A, 338 (73.2%) crashes occurred in within-intersection zone. The within-intersection zone crashes were labeled per the technique discussed in ‘Crash Labeling’ section. The labeled data were then integrated with the formatted traffic and weather dataset.

### ***Approach Integration***

In approach integration, crashes occurring only in the approach zone were labeled and integrated. In total, 124 (26.8%) crashes were identified in the approach zone.

### ***Joint Integration***

In this integration, the 432 crashes occurring both in the within-intersection zone and approach zone were labeled and integrated with the traffic and weather data.

The crash integration step generated three distinct datasets, each containing information on traffic, weather, and crash characteristics. All the datasets had the same number of observations (i.e., 280,320), however, they differed in the count of crash and non-crash events. This happened since each type of integration used different crash data sets while employing the same set of traffic and weather data.

## ***Feature Selection***

In this study, extra-tree (Geurts et al., 2006), and Pearson correlation coefficient (Benesty et al., 2009) were employed to assess feature importance and correlation. The extra-tree classifier employs a meta-estimator to fit a number of randomized decision trees on different sub-samples of the dataset and uses averaging to enhance predicted accuracy and control over-fitting (Pedregosa et al., 2012). Pearson correlation coefficient, which ranges from -1 to 1, measures the relationship between each pair of features. It expresses the intensity of a relationship between two features. A correlation is considered strong if its absolute value is more than 0.5 (Cohen, 1992).

From feature importance and correlation coefficient scores, a feature selection rule was devised. As per the rule, if two features have a correlation greater than 0.5, then the most important feature based on the feature importance score was kept for modeling. The feature selection rule

was applied on all the three datasets obtained from the ‘Crash Integration’ section. For each of the crash integration types, more than 70 features were selected from the initial 114 traffic and weather features. A list of 25 randomly selected features for each of the three integration types is presented in Table 3.

**Table 3. List of 25 Selected Features**

Crash Integration Type	Selected Features
Within-Intersection Integration	<i>‘ASM_L_A’, ‘ASA_L_A’, ‘CDM_L_A’, ‘CDA_L_A’, ‘TTM_L_B’, ‘POG_L_B’, ‘SFP_L_A’, ‘ASM_T_A’, ‘ASA_T_C’, ‘TTA_R_A’, ‘CDM_R_A’, ‘CDA_T_A’, ‘TTM_T_D’, ‘POG_T_A’, ‘ASM_L_B’, ‘ASA_L_B’, ‘ASM_T_B’, ‘CDM_L_B’, ‘CDA_L_B’, ‘TTA_L_B’, ‘TTM_L_B’, ‘CDA_T_B’, ‘TTM_T_B’, ‘POG_L_B’, precipitation</i>
Approach Integration	<i>‘ASM_L_A’, ‘CDM_T_A’, ‘CDA_L_A’, ‘TTM_L_A’, ‘POG_R_A’, ‘SFP_T_A’, ‘ASM_T_A’, ‘ASA_T_A’, ‘TTA_R_A’, ‘CDM_R_A’, ‘CDA_R_A’, ‘TTM_T_A’, ‘POG_T_A’, ‘ASM_L_A’, ‘ASA_R_A’, ‘ASM_T_A’, ‘CDM_T_A’, ‘CDA_R_A’, ‘TTA_R_A’, ‘TTM_L_A’, ‘CDA_T_A’, ‘TTM_T_A’, ‘POG_L_A’, ‘POG_T_A’, conditions</i>
Joint Integration	<i>‘ASM_L_B’, ‘ASA_L_A’, ‘CDM_C_A’, ‘CDA_L_A’, ‘TTM_T_B’, ‘POG_RL_B’, ‘SFP_L_A’, ‘ASM_T_D’, ‘ASA_T_C’, ‘TTA_R_A’, ‘CDM_R_A’, ‘CDA_T_D’, ‘TTM_T_D’, ‘POG_R_A’, ‘ASM_L_B’, ‘ASA_L_B’, ‘ASM_T_C’, ‘CDM_L_C’, ‘CDA_L_C’, ‘TTA_L_B’, ‘TTM_R_B’, ‘CDA_R_D’, ‘TTM_T_B’, ‘POG_L_B’, ‘POG_T_A’</i>

Here, A: Approach “A,” B: Approach “B,” C: Approach “C,” D: Approach “D,” and L: Left-Turn, T: Through, R: Right-Turn.

### ***Data Mapping***

The proposed inTformer, like most established deep neural networks, take three-dimensional dataset ( $batch\_size \times sequence\_length \text{ (timesteps)} \times input\_feature$ ) as input. Hence, prior to performing the analysis, the original two-dimensional timeseries data for every crash integration type was mapped to a three-dimensional dataset through data stacking. The datasets were stacked on timesteps, since previous studies (Li et al., 2022; Yuan et al., 2019; Zhang & Abdel-Aty, 2022) showed that combining 2-5 timesteps prior to crash occurrence increases the chance of accurate crash likelihood prediction. In this study, three combinations of timesteps stacking were tested, though previous studies mostly exercised a single combination. The combinations include stacking *two* ( $batch\_size \times 2 \times input\_feature$ ), *three* ( $batch\_size \times 3 \times input\_feature$ ), and *four* ( $batch\_size \times 4 \times input\_feature$ ), timesteps in data, where each timestep represents an observation in the two-dimensional dataset, and the stacked timesteps represent an observation in the three-dimensional dataset. The mapping generated a total 9 stacked datasets (3 crash integration types  $\times$  3 combinations) distinct only in crash occurrence. All the mapped datasets were independently trained to predict crashes during the next 15-30 min.

## Sampling

After data preparation and mapping, each stacked dataset per crash integration type was split into training (80%) and test (20%) datasets. The count of crash and non-crash events of training and test datasets for all combinations of crash integration type and stacking are presented in Table 4. It should be noted that the counts of crash and non-crash instances in Table 4 basically represent the count of labeled crash and non-crash events identified from the processes of crash labeling, integration, and data mapping. Hence, for a particular combination, say within-intersection integration with *two* timesteps stacked, though the initial crash count was 338 as mentioned in the ‘Crash Integration’ section and the corresponding non-crash count was 279,982 ( $280,320 - 338$ ), the processes crash labeling, integration and data mapping eventually revised the crash and non-crash counts to 676 ( $482 + 194$ ), and 273,867 ( $219,309 + 54,558$ ), respectively. In the given combination example, the reason behind the increase of crash count from 338 to 676 can be attributed to this study’s consideration on indexing two timesteps prior to occurrence of crash as crash events, as stated in the ‘Crash Labeling’ section.

**Table 4. Count of Crash and Non-Crash Events**

Crash Integration Type	Timesteps Stacked	Training Data		Test Data	
		Crash	Non-Crash	Crash	Non-Crash
Within-Intersection Integration	2	482	219,309	194	54,558
	3	482	218,652	194	54,081
	4	482	217,997	194	53,608
Approach Integration	2	186	218,123	62	54,333
	3	186	217,525	62	53,958
	4	186	216,931	62	53,585
Joint Integration	2	606	220,234	258	54,751
	3	606	219,527	258	54,191
	4	606	218,823	258	53,646

The crash-to-non-crash ratio in the training dataset, considering all combinations in Table 4, varied roughly between 1:1173 to 1:364, indicating that crash events are rare, i.e., the data is highly imbalanced. To address data imbalance, typically, majority or minority classes are often resampled, or the cost function is altered to make the misclassification of minority classes more important than the misclassification of majority classes. In this paper, the resampling technique, particularly the synthetic minority over-sampling technique (SMOTE) (Chawla et al., 2002), was employed to overcome the imbalance problem (Li et al., 2020; Yuan et al., 2019). SMOTE is an over-sampling method that generates new and synthetic data using the nearest neighbor algorithm. It creates new minority instances from existing minority instances. In this study, SMOTE was applied only on the training dataset to generate synthetic samples of crash events in a 1:1 ratio to balance crash and

non-crash events. To evaluate the crash likelihood prediction models, the unsampled test dataset was employed.

The overall data preparation pipeline of this study is depicted in Figure 5.

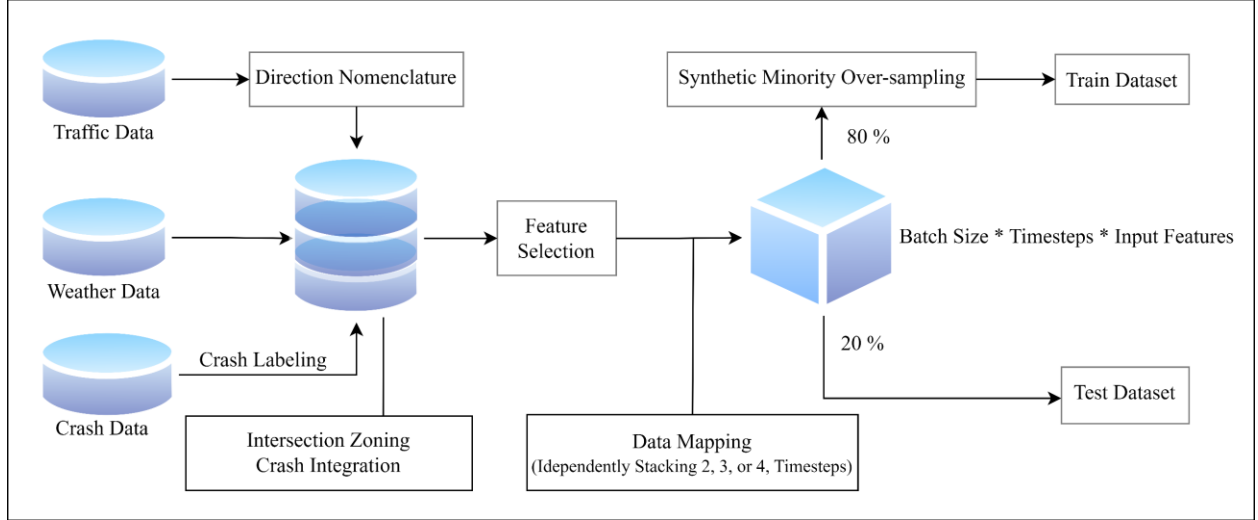


**Figure 5. Data Preparation Pipeline**

## METHODOLOGY

In this study, five distinct methods: LSTM, CNN, sequential LSTM-CNN, parallel LSTM-CNN, and the proposed inTersection-Transformer (i.e., inTformer), were employed to develop the real-time crash likelihood prediction models. All models were trained using the synthetic train dataset. In the end, the five developed real-time crash prediction models were evaluated on the same unsampled test dataset.

### LSTM

The LSTM architecture (Hochreiter & Schmidhuber, 1997) is a recurrent neural network (RNN) architecture designed to model sequential input. Previously, traditional RNNs experienced vanishing gradient problems when learning large data sequences (Arbel, 2018). LSTM, by incorporating the memory cell to determine when to forget certain information, could solve this problem.

The LSTM network employs a series of connected cells. An input gate  $i_t$ , a forget gate  $f_t$ , an output gate  $o_t$ , a memory cell  $c_t$ , and a hidden state  $h_t$ , comprises a standard LSTM cell. The input and forget gates determine how much information is drawn from the current timestep features  $x_t$  and how much information is drawn from the preceding cell hidden state  $h_{t-1}$ . The output gate determines how much information is transferred to the next cell by calculating the current cell's



hidden state  $h_t$ . The calculations performed by each LSTM cell at timestep  $t$  are specified in Equations 2-7 (Graves et al., 2013). The computations are carried out for each member of the modeled sequence  $t = 0 \dots T$ .

$$i_t = \sigma(W_{ix}X_t + W_{ih}h_{t-1} + W_{ic}c_{t-1} + b_i) \quad (2)$$

$$f_t = \sigma(W_{fx}X_t + W_{fh}h_{t-1} + W_{fc}c_{t-1} + b_f) \quad (3)$$

$$o_t = \sigma(W_{ox}X_t + W_{oh}h_{t-1} + W_{oc}c_{t-1} + b_o) \quad (4)$$

$$c_t = f_t \odot c_{t-1} + i_t \odot \tanh(W_{cx}X_t + W_{ch}h_{t-1} + b_c) \quad (5)$$

$$h_t = o_t \odot \tanh(c_t) \quad (6)$$

$$y_t = W_{yh}h_{t-1} + b_y \quad (7)$$

where  $W$ , and  $b$  represents network trainable weight matrices, and bias vectors, respectively.  $\sigma$  is the logistic sigmoid function, and  $\odot$  indicates the elementwise product of the vectors.

## CNN

CNN was first designed to address image classification challenges. Recently, multiple studies suggested that CNN may also be leveraged to learn time-series data with promising results (Wang et al., 2016; Zhao et al., 2017). The convolution layer of CNN employs a filter to extract features from the input data (Fawaz et al., 2019). As a feature extractor, this work used a one-dimensional (1D) CNN using Rectified Linear Unit (ReLU) as the activation function. The capacity of CNN to learn features that are invariant across time dimensions is one advantage of employing it for time-series data. Moreover, previous studies (Li et al., 2020; Li & Abdel-Aty, 2022) also validated the possibility of utilizing CNN for crash likelihood prediction.

## inTersection-Transformer / inTformer

Originally, the Transformer algorithm was designed to perform NLP tasks leveraging attention-mechanism (Vaswani et al., 2017). In this study, the functional domain of the original transformer is extended to predict crash likelihood in real-time at intersections. The proposed inTersection-Transformer (inTformer) architecture employed in this paper is depicted in Figure 6. The inTformer requisites normalized sequential data in dimension  $\text{batch\_size} \times \text{sequence\_length (timesteps)} \times \text{input\_feature}$  as input. A brief description of each layer in Figure 6 is summarized below.

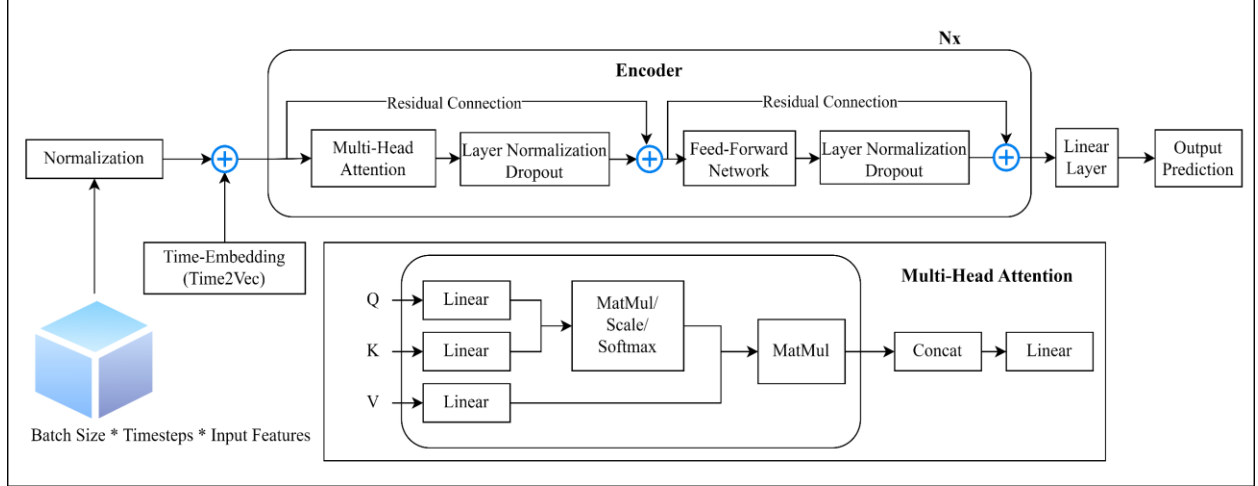


**Figure 6. inTformer Architecture**

### ***Time Embedding***

In Transformers, all data is forwarded all at once through the model architecture to learn dependencies and interactions in the sequential data. Hence, unlike traditional RNNs and LSTM models, Transformers structurally favor an attention-based system by averting sequential processing. Though the attention-based system can identify dependencies in almost every type of sequential data, at times the inability of sequential processing makes it difficult for Transformer to extract dependencies in data with a time sequence (i.e., time series data). Since real-time crash likelihood prediction requires time series data as input, in this study a serious sequential challenge was posed while developing the inTformer architecture. This sequential issue was resolved by embedding a ‘Time Embedding’ layer in the inTformer architecture that could account for the temporal order of the data sequence to predict crash within the next 15-30 min.

In the inTformer architecture, the ‘Time Embedding’ layer was formulated by adopting the model-agnostic time representation, also called ‘Time2Vec,’ approach proposed by Kazemi et al. (2019). In accordance with the principles proposed in ‘Time2Vec,’ two ideas were implemented in the ‘Time Embedding’ layer: *firstly*, a realistic depiction of time must incorporate periodic and nonperiodic patterns, and *secondly*, a time depiction should be invariant to time rescaling, which means that it is unaffected by varied time increments (i.e., seconds, hours, or days) and long-time horizons. The mathematical definition attained by combining the ideas is presented below (Equation 8).

$$t2v(\tau)[i] = \begin{cases} \omega_i \tau + \varphi_i, & i = 0 \\ F(\omega_i \tau + \varphi_i), & 1 \leq i \leq k \end{cases} \quad (8)$$

where  $\omega_i \tau + \varphi_i$  represents the non-periodic/linear and  $F(\omega_i \tau + \varphi_i)$  the periodic feature of the time vector.  $\omega$  in  $\omega_i \tau + \varphi_i$  is a matrix that defines the slope of time-series  $\tau$  and  $\varphi$  in simple terms

is a matrix that defines where the time-series  $\tau$  intersects with the y-axis.  $F(\cdot)$  is a function that makes the linear term  $\omega_i\tau + \varphi_i$  periodic.

### **Encoder**

The ‘Encoder’ layer is the core layer of the proposed inTformer. In the seminal paper (Vaswani et al., 2017), the proposed Transformer had two core layers: Encoder and Decoder. However, in this paper, the inTformer focused on leveraging only the functionality of the former to predict crash likelihood at intersections. The proposed inTformer architecture can have multiple ‘Encoder’ layers, and each ‘Encoder’ layer incorporates two key sub-layers: Multi-Head Attention Mechanism, and Position-Wise Feed-Forward Network.

#### *Multi-Head Attention Mechanism*

This sub-layer executes the attention mechanism of the inTformer by concatenating the attention weights of single heads. Each single-head takes three inputs, namely query  $Q$ , key  $K$ , and value  $V$ , in total to calculate the attention weights that measure the relationship between elements/inputs in a sequence. The  $Q$ ,  $K$ , and  $V$  vectors are obtained by transforming each input from a sequence of inputs (in our case, a sequence of time-embedded inputs).

Say,  $X = [x_1, x_2, x_3, \dots, x_n]$  represents time-embedded input sequences, where  $x_i$  is the input at timestep  $i$ . The input  $x_i$  can be transformed into three vectors as follows (Equation 9):

$$Q_i = x_i W_q; K_i = x_i W_k; V = x_i W_v \quad (9)$$

where  $W_q$ ,  $W_k$ , and  $W_v$  are weight matrices for the query, key, and value transformations, respectively, which are learned during training. After the  $Q$ ,  $K$ , and  $V$  vectors of all timesteps have been determined, the attention scores are then computed for each pair of  $Q$  and  $K$  vectors. Specifically, for  $Q_i$  and  $K_j$  (corresponding to timesteps  $i$  and  $j$ ), the score is calculated as the dot product of  $Q_i$  and  $K_j$  as follows (Equation 10):

$$S_{ij} = Q_i K_j^{Transpose} \quad (10)$$

The attention score  $S_{ij}$  measures the similarity between the  $Q$  and  $K$ , effectively determining how much attention should be paid from  $Q_i$  (query at time step  $i$ ) to  $K_j$  (key at time step  $j$ ). The raw attention scores are then normalized using a ‘softmax’ function to ensure that they sum up to one across all time steps for each  $Q$ . Also, the scores are usually scaled down by the square root of the dimension of the key vectors  $d_k$  to avoid extremely large values, which could lead to unstable gradients as follows (Equation 11):

$$A_{ij} = \text{Softmax}\left(\frac{S_{ij}}{\sqrt{d_k}}\right) \quad (11)$$

For each single-head, using the attention weights, outputs for each input  $x_i$  are computed as a weighted sum of the  $V$  vectors (Equation 12). Finally, the output matrices from all the  $h$  single-heads are then concatenated (Equation 13) and passed through a final linear transformation (Equation 14).

$$O_i = \sum_j A_{ij} \times V_j, \quad j = 1, 2, \dots, n \text{ including timestep } i \quad (12)$$

$$O_{concat} = \text{concat}(O_1, O_2, \dots, O_h) \quad (13)$$

$$O_{final} = \text{linear}(O_{concat}) \quad (14)$$

The final output vectors  $O_{final}$  form the output sequence of the multi-head attention mechanism.

#### *Position-Wise Feed-Forward Network*

The purpose of this sub-layer is to transform the representation received from the ‘Multi-Head Attention Mechanism,’ allowing the model to identify more complex relationships. The term “position-wise” in ‘Position-Wise Feed-Forward Network’ refers to the fact that the same Feed-Forward Network is applied separately to each input in a sequence of inputs (in our case, a sequence of time-embedded inputs). This is analogous to using a convolution with a kernel size of 1 in CNN. As a result, CNN with convolution kernel size 1 was incorporated into the inTformer architecture as a ‘Position-Wise Feed-Forward Network.’ The CNN used in inTformer’s ‘Encoder’ includes two layers, which are as follows:

1. In the *first* layer, initially a simple linear transformation takes place that projects (increases) the dimension of input data to a higher dimensional space. Following the linear transformation, an element-by-element application of a non-linear activation function (in our example, ReLU) is performed.
2. In the *second* layer, the output from the activation function is then passed through a second linear transformation, which projects the data back to the original dimension.

In ‘Encoder,’ each of the key sub-layers: ‘Multi-Head Attention Mechanism’ and ‘Position-Wise Feed-Forward Network,’ are followed by dropout, residual connection, and layer normalization. The inclusion of dropout helps prevent the model from overfitting by not allowing it to rely too heavily on any single input/element in the sequence. The residual connections, also known as skip or shortcut connections, help the inTformer combat the problem of vanishing gradients. Layer normalization is a process that normalizes the values of the activations in a layer to have a mean of 0 and a variance of 1. This helps keep the activations and gradients on a similar scale, leading to more stable training. In inTformer, layer normalization helps ensure that the scale of the values throughout the model doesn’t get out of control, which can lead to issues with learning.

## Performance Metrics

In general, several key metrics, such as accuracy, sensitivity, false positive rate, etc., are utilized to evaluate model performance. While accuracy is often assessed for balanced datasets, model performance for imbalanced datasets is frequently measured using metrics such as sensitivity, false alarm rate, and so on. Hence, in this study, sensitivity, and false alarm rate were employed for model performance evaluation using test dataset. Sensitivity (Equation 15) and false alarm rate (Equation 16) are derived from the classification confusion matrix (Table 5). The sensitivity reflects the percentage of correct positive predictions produced (Raihan et al., 2023; Syed et al., 2023), whereas the false positive rate indicates how frequently the model is likely to mispredict.

**Table 5. Confusion Matrix**

		Predicted Label	
		Crash	Non-Crash
Actual Label	Crash	True Positive (TP)	False Negative (FN)
	Non-Crash	False Positive (FP)	True Negative (TN)

$$\text{True Positive Rate (Sensitivity)} = \frac{TP}{TP + FN} \quad (15)$$

$$\text{False Positive Rate (False Alarm Rate)} = \frac{FP}{FP + TN} \quad (16)$$

## RESULTS

### Hyperparameter Tuning

A crucial step to achieving reliable results from the model training is to tune hyperparameters and select appropriate optimization functions. Hence, in this study, all the inTformer models were tuned from a pool of hyperparameters and optimization functions presented in Table 6.

**Table 6. Pool of Parameters for Hyperparameter Tuning**

Hyperparameter	Range
Learning Rate	0.00001, 0.0001, 0.001, 0.01
Batch Size	500, 1000, 2500, 5000, 10000
Epoch Number	50, 100, 150, 200, 250
No. of Heads	3, 5, 8
No. of Encoders	1, 2, 3, 4, 5
Optimization Function	Adam, RMSprop, SGD

## Model Evaluation

In this study, the original dataset was simultaneously mapped to nine sets of three-dimensional datasets through crash integration and stacking data on timesteps. To do so, the original dataset was independently formatted on three crash integration types: within-intersection integration, approach integration, and joint integration, and stacked on *two*, *three*, and *four*, timesteps, respectively. The inTformer algorithm was separately trained on each of the train datasets extracted from the nine mapped datasets. To evaluate the performance of the models, the nine retrieved test datasets from mapped datasets (see Table 4) were employed. The sensitivity and false alarm rate of all the developed inTformer models are presented in Table 7.

**Table 7. Experiment Results of inTformer per Stacking**

Models	Performance Scores	
	Sensitivity	False Alarm Rate
inTformer (Type A + II)	0.71	0.36
inTformer (Type A + III)	0.64	0.38
inTformer (Type A + IV)	0.66	0.44
inTformer (Type B + II)	0.70	0.37
inTformer (Type B + III)	0.64	0.39
inTformer (Type B + IV)	0.66	0.42
inTformer (Type C + II)	<b>0.73</b>	<b>0.35</b>
inTformer (Type C + III)	0.68	0.41
inTformer (Type C + IV)	0.65	0.39

Here, Type A: within-intersection integration, Type B: approach integration, and Type C: joint integration, and II, III and IV stands for stacking on *two*, *three* and *four*, timesteps, respectively.

The result in Table 7 shows that inTformer (Type C + II) model i.e., inTformer model trained on dataset through joint crash integration and stacking *two* timesteps, performed better than all other developed inTformer models. The confusion matrix generated from testing inTformer (Type C + II) model on the respective test data is depicted in Table 8.

**Table 8. Confusion Matrix of the inTformer (Type C + II) Model**

		Predicted Label	
		Crash	Non-Crash
Actual Label	Crash	185	73
	Non-Crash	20,909	37,170

## Model Comparison

To check the performance of the inTformer model, several established deep neural networks, namely LSTM, CNN, sequential LSTM-CNN, parallel LSTM-CNN, were also trained and tested on the same respective mapped datasets. All the compared models were fine-tuned accordingly. Figure 7 presents the comparison results of inTformer (Type C + II) model with all the established models trained in this study. The comparison results verify that the inTformer (Type C + II) has the highest sensitivity and lowest false alarm rate compared to other established models developed in this study. This finding proves the suitability of employing inTformer model in real-time crash likelihood prediction at intersections.

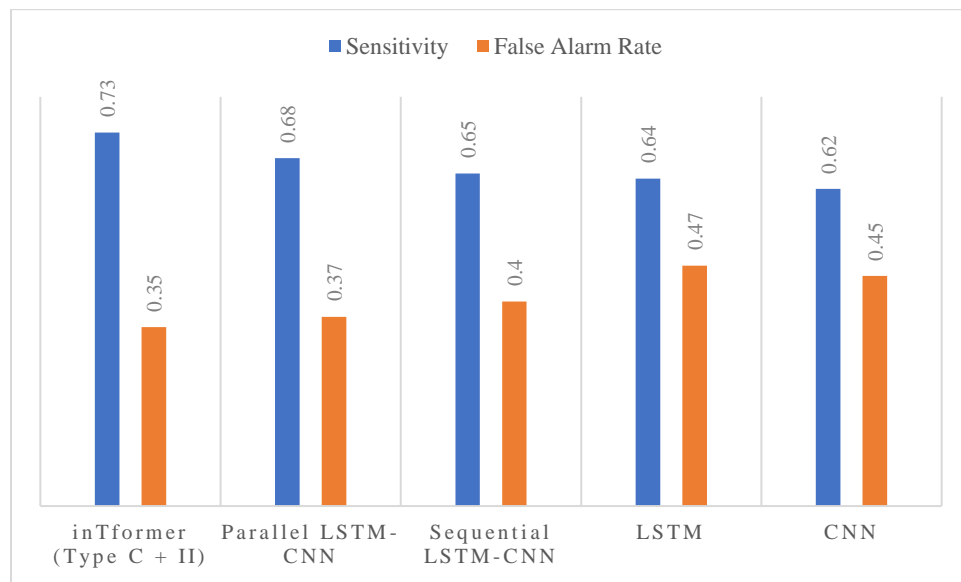


**Figure 7. Model Comparison Results**

Furthermore, the performance of the proposed inTformer was tested with the findings of previous studies on real-time crash likelihood prediction at intersections using deep learning neural networks. To the best of the author's knowledge, only Yuan et al. (2019) applied a deep learning model, namely LSTM, to predict crash likelihood in real-time at intersections. The comparison of inTformer (Type C + II) with the proposed LSTM by Yuan et al. (2019) is presented in Table 9.

**Table 9. Model Comparison with Previous Studies**

Models	Performance Scores	
	Sensitivity	False Alarm Rate
inTformer (Type C + II)	<b>0.73</b>	<b>0.35</b>
Yuan et al. (2019)	0.61	0.39

Table 9 supports the superiority of the proposed inTformer model in real-time crash likelihood prediction at intersections.

## CONCLUSIONS

In this paper, the authors proposed inTformer, a time-embedded attention-based Transformer that can predict intersection crash likelihood in real-time. In order to develop the model, data from three distinct sources, namely crash data from S4A, connected vehicle data (representing traffic dynamics at intersections) from Signal Analytics, and weather data, were combined and formatted in accordance with a previously proposed nomenclature (Yuan & Abdel-Aty, 2018). The formatting resulted in an unbalanced time-series dataset in which each timestep characterized the traffic dynamics of all approaches to an intersection as well as information on multiple weather parameters. To balance the data and ensure no non-crash information is lost during training, the synthetic minority oversampling technique (SMOTE) was employed on the training dataset prior to forwarding it as an input to the inTformer model.

The traffic behavior within an intersection is quite different from that of the approaches to an intersection, resulting in complex crash occurrence mechanism. To account for such complexity, in this research, the study intersections were segmented into zones prior to crash likelihood prediction. Moreover, based on previous studies, which indicated merging 2-5 timesteps prior to the occurrence of a crash improves the accuracy of crash likelihood prediction, data mapping through stacking on timesteps was implemented. A total of nine independent datasets were generated combining both the zoning and mapping strategies. The inTformer algorithm was separately trained and tested on each of the mapped datasets producing nine different models. The prediction results indicated that inTformer (Type C + II) was better in real-time crash likelihood prediction at intersections. The inTformer (Type C + II) model can predict 73% of the intersection crashes with a false alarm rate of 35%. This finding confirms that, when using connected vehicle data taken from Signal Analytics, the inTformer method is more effective in predicting crash likelihood, if crashes occurring within the intersection and at the approaches to the intersection are accounted for jointly, i.e., Type C integration.

Typically, from a traffic point of view, crash likelihood prediction models based on Type A integration or Type B integration should have better predictive performance, since these types of models analyze crashes within the intersection and at the approach to the intersection separately. However, in this study, the inTformer model, which modeled crashes both within the intersection and at the approach to the intersection jointly, turned out to be more effective. The explanation for this finding is the way INRIX and CATT Lab archives traffic data in the Signal Analytics platform. As previously mentioned in the ‘Data Description’ section, Signal Analytics measures traffic features using the pings collected from connected vehicles as they traverse a 230-meter intersection zone. The measurements of all features, however, do not take into account the collected pings from the entire 230-meter zone. For instance, the Signal Analytics platform measures approach speed using pings from the 150-meter approach zone, while it measures travel time using pings from the



entire 230-meter zone, which includes both the within-intersection zone and the approach zone (see Figures 1-2). As the features estimated by the Signal Analytics platform collectively represent the traffic dynamics of both the within-intersection zone and the approach zone, they hold immense potential for jointly modeling the crash mechanisms within the intersection and on the approach. In other words, by employing features like approach speed, travel time, and others from the Signal Analytics platform, crashes occurring both within the intersection and on its approach can be analyzed jointly. The enhanced performance of the inTformer (Type C + II) model in this study serves as a clear testament to this fact.

The inTformer model is evidence of the first attempt to implement a time-embedded attention-based Transformer to predict crash likelihood at intersections in real-time. Considering the fact that traffic operation mechanisms at intersections are very complex, the result obtained from the inTformer is quite reasonable. The inTformer model, particularly inTformer (Type C + II), not only performed better than multiple established deep learning models trained on the same dataset, but also outperformed previously proposed deep neural networks (Yuan et al., 2019), in predicting intersection crash likelihood in real-time. In addition to identifying the aptness of Transformer in crash likelihood prediction, this study also confirms that Signal Analytics' connected vehicle data, which accounts for intersection traffic dynamics, can be considered a suitable source of traffic data for real-time crash likelihood prediction at intersections.

In summary, this paper succeeds in verifying the viability of real-time crash likelihood prediction at intersections using the proposed inTformer with SMOTE over-sampling. The results of the inTformer model indicate its suitability for the implementation of an advanced traffic management system that has the potential to reduce crashes. Nevertheless, the current research has several unexplored directions. Firstly, embedding extra layers in the inTformer architecture or tuning the inTformer on additional hyperparameter combinations. Secondly, resampling techniques other than SMOTE or data augmentation can be implemented to check out the possibility of enhanced model performance. Finally, driver characteristics extracted from connected vehicles, such as hard braking, hard acceleration, etc., can be incorporated into model training, since it has been extensively exhibited that crash events are highly prompted by driver characteristics and driving behavior prior to crash occurrence.

## REFERENCES

- Abdel-Aty, M., & Wang, X. (2006). Crash Estimation at Signalized Intersections along Corridors. *Transportation Research Record: Journal of the Transportation Research Board*, 1953(1), 98–111. <https://doi.org/10.1177/0361198106195300112>
- Abdel-Aty, M., Zheng, O., Wu, Y., Abdelraouf, A., Rim, H., & Li, P. (2023). Real-Time Big Data Analytics and Proactive Traffic Safety Management Visualization System. *Journal of Transportation Engineering, Part A: Systems*, 149(8). <https://doi.org/10.1061/JTEPBS-TEENG-7530>
- Abdelraouf, A., Abdel-Aty, M., & Wu, Y. (2022). Using Vision Transformers for Spatial-Context-Aware Rain and Road Surface Condition Detection on Freeways. *IEEE Transactions on Intelligent Transportation Systems*, 23(10), 18546–18556. <https://doi.org/10.1109/TITS.2022.3150715>
- Ahmed, A. J. M. M. U., Hasan, M. T., Alam, M. R., & Hoque, M. S. (2017). Characteristics of Fundamental Diagrams Due to Shockwave by Non-Lane Based Heterogeneous Traffic. *Proceedings of International Structural Engineering and Construction*, 4(1). <https://doi.org/10.14455/ISEC.res.2017.112>
- Ahmed, M. M., & Abdel-Aty, M. A. (2012). The viability of using automatic vehicle identification data for real-time crash prediction. *IEEE Transactions on Intelligent Transportation Systems*, 13(2), 459–468. <https://doi.org/10.1109/TITS.2011.2171052>
- Ahsan, M. J., Roy, S., & Huq, A. S. (2021). An In-Depth Estimation of Road Traffic Accident Cost in Bangladesh. *Proceedings of the International Conference on Sustainable Development in Technology for 4th Industrial Revolution 2021 (ICSDTIR-2021)*. <https://www.researchgate.net/publication/350443292>
- Ali, Y., Washington, S., & Haque, M. M. (2023). Estimating real-time crash risk at signalized intersections: A Bayesian Generalized Extreme Value approach. *Safety Science*, 164, 106181. <https://doi.org/10.1016/j.ssci.2023.106181>
- Arbel, N. (2018). *How LSTM networks solve the problem of vanishing gradients*. Medium. <https://medium.datadriveninvestor.com/how-do-lstm-networks-solve-the-problem-of-vanishing-gradients-a6784971a577>
- Basso, F., Pezoa, R., Varas, M., & Villalobos, M. (2021). A deep learning approach for real-time crash prediction using vehicle-by-vehicle data. *Accident Analysis and Prevention*, 162. <https://doi.org/10.1016/j.aap.2021.106409>
- Benesty, J., Chen, J., Huang, Y., & Cohen, I. (2009). Pearson correlation coefficient. *Springer Topics in Signal Processing*, 2, 1–4. [https://doi.org/10.1007/978-3-642-00296-0\\_5/COVER](https://doi.org/10.1007/978-3-642-00296-0_5/COVER)
- Chawla, N. V., Bowyer, K. W., Hall, L. O., & Kegelmeyer, W. P. (2002). SMOTE: Synthetic Minority Over-sampling Technique. *Journal of Artificial Intelligence Research*, 16, 321–357. <https://doi.org/10.1613/JAIR.953>
- Cheng, Z., Yuan, J., Yu, B., Lu, J., & Zhao, Y. (2022). Crash Risks Evaluation of Urban Expressways: A Case Study in Shanghai. *IEEE Transactions on Intelligent Transportation Systems*, 23(9), 15329–15339. <https://doi.org/10.1109/TITS.2022.3140345>
- Cohen, J. (1992). A power primer. *Psychological Bulletin*, 112(1), 155–159. <https://doi.org/10.1037/0033-2909.112.1.155>

- Devlin, J., Chang, M.-W., Lee, K., & Toutanova, K. (2018). *BERT: Pre-training of Deep Bidirectional Transformers for Language Understanding*. <http://arxiv.org/abs/1810.04805>
- Geurts, P., Ernst, D., & Wehenkel, L. (2006). Extremely randomized trees. *Machine Learning*, 63(1), 3–42. <https://doi.org/10.1007/S10994-006-6226-1/METRICS>
- Graves, A., Mohamed, A. R., & Hinton, G. (2013). Speech Recognition with Deep Recurrent Neural Networks. *ICASSP, IEEE International Conference on Acoustics, Speech and Signal Processing - Proceedings*, 6645–6649. <https://doi.org/10.1109/ICASSP.2013.6638947>
- Gulati, A., Qin, J., Chiu, C.-C., Parmar, N., Zhang, Y., Yu, J., Han, W., Wang, S., Zhang, Z., Wu, Y., & Pang, R. (2020). *Conformer: Convolution-augmented Transformer for Speech Recognition*. <http://arxiv.org/abs/2005.08100>
- Guo, F., Wang, X., & Abdel-Aty, M. A. (2010). Modeling signalized intersection safety with corridor-level spatial correlations. *Accident Analysis and Prevention*, 42(1), 84–92. <https://doi.org/10.1016/j.aap.2009.07.005>
- Guo, S., Lin, Y., Feng, N., Song, C., & Wan, H. (2019). Attention Based Spatial-Temporal Graph Convolutional Networks for Traffic Flow Forecasting. *Proceedings of the AAAI Conference on Artificial Intelligence*, 33(01), 922–929. <https://doi.org/10.1609/aaai.v33i01.3301922>
- Hasan, T., Abdel-Aty, M., & Mahmoud, N. (2022). Freeway Crash Prediction Models with Variable Speed Limit/Variable Advisory Speed. *Journal of Transportation Engineering, Part A: Systems*, 149(3), 04022159. <https://doi.org/10.1061/JTEPBS.TEENG-7349>
- Hochreiter, S., & Schmidhuber, J. (1997). Long Short-Term Memory. *Neural Computation*, 9(8), 1735–1780. <https://doi.org/10.1162/NECO.1997.9.8.1735>
- Hossain, M., Abdel-Aty, M., Quddus, M. A., Muromachi, Y., & Sadeek, S. N. (2019). Real-time crash prediction models: State-of-the-art, design pathways and ubiquitous requirements. *Accident Analysis and Prevention*, 124, 66–84. <https://doi.org/10.1016/j.aap.2018.12.022>
- Islam, Z., Abdel-Aty, M., Cai, Q., & Yuan, J. (2021). Crash data augmentation using variational autoencoder. *Accident Analysis and Prevention*, 151. <https://doi.org/10.1016/j.aap.2020.105950>
- Ismail Fawaz, H., Forestier, G., Weber, J., Idoumghar, L., & Muller, P. A. (2019). Deep learning for time series classification: a review. *Data Mining and Knowledge Discovery*, 33(4), 917–963. <https://doi.org/10.1007/S10618-019-00619-1/FIGURES/16>
- Kazemi, S. M., Goel, R., Eghbali, S., Ramanan, J., Sahota, J., Thakur, S., Wu, S., Smyth, C., Poupart, P., & Brubaker, M. (2019). *Time2Vec: Learning a Vector Representation of Time*. <http://arxiv.org/abs/1907.05321>
- Kidando, E., Kitali, A. E., Kutela, B., Karaer, A., Ghorbanzadeh, M., Koloushani, M., & Ozguven, E. E. (2022). Use of Real-Time Traffic and Signal Timing Data in Modeling Occupant Injury Severity at Signalized Intersections. *Transportation Research Record*, 2676(2), 825–839. <https://doi.org/10.1177/03611981211047836>
- Lee, J., Abdel-Aty, M., & Cai, Q. (2017). Intersection crash prediction modeling with macro-level data from various geographic units. *Accident Analysis and Prevention*, 102, 213–226.

<https://doi.org/10.1016/j.aap.2017.03.009>

- Li, P., & Abdel-Aty, M. (2022). Real-Time Crash Likelihood Prediction Using Temporal Attention-Based Deep Learning and Trajectory Fusion. *Journal of Transportation Engineering, Part A: Systems*, 148(7). <https://doi.org/10.1061/jtepbs.0000697>
- Li, P., Abdel-Aty, M., & Yuan, J. (2020). Real-time crash risk prediction on arterials based on LSTM-CNN. *Accident Analysis and Prevention*, 135. <https://doi.org/10.1016/j.aap.2019.105371>
- Li, P., Abdel-Aty, M., & Zhang, S. (2022). Improving Spatiotemporal Transferability of Real-Time Crash Likelihood Prediction Models Using Transfer-Learning Approaches. *Transportation Research Record*, 2676(11), 621–631. <https://doi.org/10.1177/03611981221094289>
- Lin, L., Wang, Q., & Sadek, A. W. (2015). A novel variable selection method based on frequent pattern tree for real-time traffic accident risk prediction. *Transportation Research Part C: Emerging Technologies*, 55, 444–459. <https://doi.org/10.1016/j.trc.2015.03.015>
- Pedregosa, F., Varoquaux, G., Gramfort, A., Michel, V., Thirion, B., Grisel, O., Blondel, M., Prettenhofer, P., Weiss, R., Dubourg, V., Vanderplas, J., Passos, A., Cournapeau, D., Brucher, M., Perrot, M., & Duchesnay, É. (2012). Scikit-learn: Machine Learning in Python. *Journal of Machine Learning Research*, 12, 2825–2830. <https://arxiv.org/abs/1201.0490v4>
- Raihan, M. A., Anik, B. M., Ashik, F. R., Hasan, M. M., & Mahmud, M. M. (2023). Motorcycle Helmet Use Behavior: What Does Our Data Tell Us?
- Rashid, M., Ahmed, S., Kalam, N., Anik, M., & Hossain, M. (2018). Evaluation of public bus comfort in Dhaka city. *Proceedings of the 4th International Conference on Advances in Civil Engineering*.
- Shi, Q., & Abdel-Aty, M. (2015). Big Data applications in real-time traffic operation and safety monitoring and improvement on urban expressways. *Transportation Research Part C: Emerging Technologies*, 58, 380–394. <https://doi.org/10.1016/j.trc.2015.02.022>
- Shi, Q., Abdel-Aty, M., & Yu, R. (2016). Multi-level Bayesian safety analysis with unprocessed Automatic Vehicle Identification data for an urban expressway. *Accident Analysis and Prevention*, 88, 68–76. <https://doi.org/10.1016/j.aap.2015.12.007>
- Signal Analytics Help. (n.d.). Retrieved June 18, 2023, from <https://signals.ritis.org/analytics/help/#intersection-matrix>
- Syed, Z. E. M., Hasan, S., & Syed, H. (2023). *Predicting Real-time Crash Risks during Hurricane Evacuation Using Connected Vehicle Data*. <https://arxiv.org/abs/2306.08682v1>
- Theofilatos, A. (2017). Incorporating real-time traffic and weather data to explore road accident likelihood and severity in urban arterials. *Journal of Safety Research*, 61, 9–21. <https://doi.org/10.1016/j.jsr.2017.02.003>
- Theofilatos, A., Chen, C., & Antoniou, C. (2019). Comparing Machine Learning and Deep Learning Methods for Real-Time Crash Prediction. *Transportation Research Record*, 2673(8), 169–178. <https://doi.org/10.1177/0361198119841571>
- Vaswani, A., Shazeer, N., Parmar, N., Uszkoreit, J., Jones, L., Gomez, A. N., Kaiser, Ł., &

- Polosukhin, I. (2017). Attention is all you need. *Advances in Neural Information Processing Systems, 2017-Decem*, 5999–6009. <https://doi.org/https://doi.org/10.48550/arXiv.1706.03762>
- Wang, Z., Yan, W., & Oates, T. (2016). Time Series Classification from Scratch with Deep Neural Networks: A Strong Baseline. *Proceedings of the International Joint Conference on Neural Networks, 2017-May*, 1578–1585. <https://doi.org/10.1109/IJCNN.2017.7966039>
- Wu, Y., Guo, Y., & Yin, W. (2021). Real time safety model for pedestrian red-light running at signalized intersections in China. *Sustainability (Switzerland)*, 13(4), 1–11. <https://doi.org/10.3390/su13041695>
- Xu, M., Dai, W., Liu, C., Gao, X., Lin, W., Qi, G.-J., & Xiong, H. (2020). *Spatial-Temporal Transformer Networks for Traffic Flow Forecasting*. <http://arxiv.org/abs/2001.02908>
- You, J., Wang, J., & Guo, J. (2017). Real-time crash prediction on freeways using data mining and emerging techniques. *Journal of Modern Transportation*, 25(2), 116–123. <https://doi.org/10.1007/s40534-017-0129-7>
- Yu, R., & Abdel-Aty, M. (2013). Utilizing support vector machine in real-time crash risk evaluation. *Accident Analysis and Prevention*, 51, 252–259. <https://doi.org/10.1016/j.aap.2012.11.027>
- Yu, R., & Abdel-Aty, M. (2014). Analyzing crash injury severity for a mountainous freeway incorporating real-time traffic and weather data. *Safety Science*, 63, 50–56. <https://doi.org/10.1016/j.ssci.2013.10.012>
- Yu, R., Wang, Y., Zou, Z., & Wang, L. (2020). Convolutional neural networks with refined loss functions for the real-time crash risk analysis. *Transportation Research Part C: Emerging Technologies*, 119. <https://doi.org/10.1016/j.trc.2020.102740>
- Yuan, J., & Abdel-Aty, M. (2018). Approach-level real-time crash risk analysis for signalized intersections. *Accident Analysis and Prevention*, 119, 274–289. <https://doi.org/10.1016/j.aap.2018.07.031>
- Yuan, J., Abdel-Aty, M. A., Yue, L., & Cai, Q. (2021). Modeling Real-Time Cycle-Level Crash Risk at Signalized Intersections Based on High-Resolution Event-Based Data. *IEEE Transactions on Intelligent Transportation Systems*, 22(11), 6700–6715. <https://doi.org/10.1109/TITS.2020.2994126>
- Yuan, J., Abdel-Aty, M., Gong, Y., & Cai, Q. (2019). Real-Time Crash Risk Prediction using Long Short-Term Memory Recurrent Neural Network. *Transportation Research Record*, 2673(4), 314–326. <https://doi.org/10.1177/0361198119840611>
- Yuan, J., Abdel-Aty, M., Wang, L., Lee, J., Yu, R., & Wang, X. (2018). Utilizing bluetooth and adaptive signal control data for real-time safety analysis on urban arterials. *Transportation Research Part C: Emerging Technologies*, 97, 114–127. <https://doi.org/10.1016/j.trc.2018.10.009>
- Zhang, S., & Abdel-Aty, M. (2022). Real-time crash potential prediction on freeways using connected vehicle data. *Analytic Methods in Accident Research*, 36. <https://doi.org/10.1016/j.amar.2022.100239>
- Zhao, B., Lu, H., Chen, S., Liu, J., & Wu, D. (2017). Convolutional neural networks for time series

classification. *Journal of Systems Engineering and Electronics*, 28(1), 162–169. <https://doi.org/10.21629/JSEE.2017.01.18>

Zheng, L., & Sayed, T. (2020). A novel approach for real time crash prediction at signalized intersections. *Transportation Research Part C: Emerging Technologies*, 117. <https://doi.org/10.1016/j.trc.2020.102683>

Zheng, Q., Xu, C., Liu, P., & Wang, Y. (2021). Investigating the predictability of crashes on different freeway segments using the real-time crash risk models. *Accident Analysis and Prevention*, 159. <https://doi.org/10.1016/j.aap.2021.106213>